

Supplemental Material

Contents: Supplemental Figures S1-S11

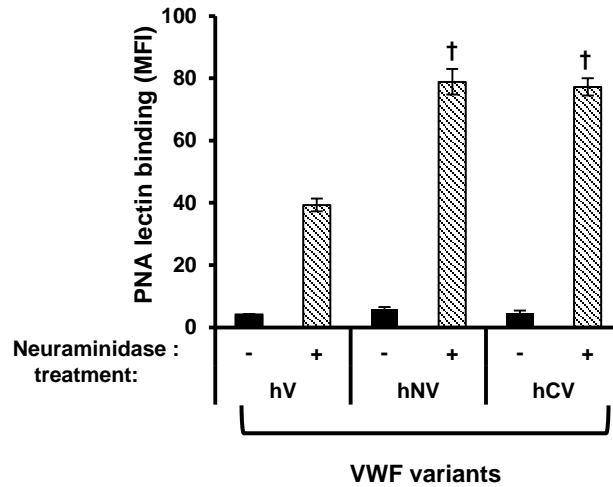


Figure S1. Peanut agglutinin binding to immobilized VWF: 10µg/mL VWF proteins were captured on anti-VWF beads. 200U/ml *A. ureafaciens* α2-3,6,8,9 Neuraminidase A (New England Biolabs) was added in some cases for 1h at 37°C to remove sialic acids and expose the T-antigen (Galβ1,3GalNAc) prior to capture on anti-VWF beads. Peanut agglutinin-FITC (1:100 dilution from Vector labs) binding to beads was then measured. This lectin binds the Galβ1,3GalNAcα epitope on desialylated O-linked glycans. Insertion of mucin-repeat in hNV and hCV doubles the amount of Peanut agglutinin-FITC binding. Equivalent amounts of total VWF was captured in each case. Overall, the CD43 mucin insert increases the prevalence of O-glycans on VWF. † $P < 0.05$ with respect to hV protein.

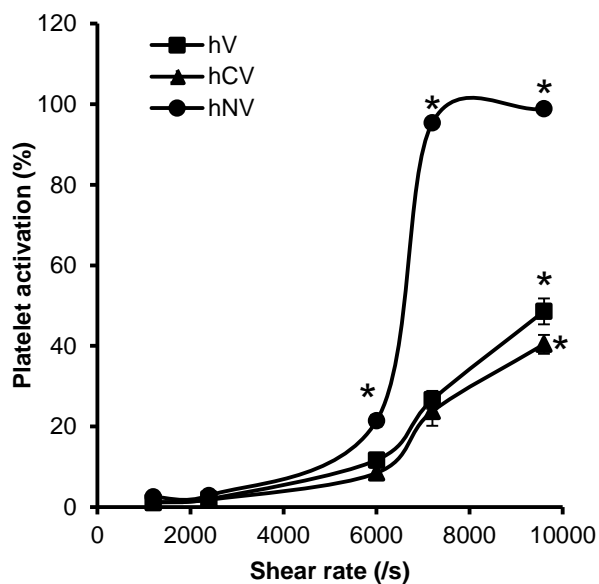


Figure S2. SIPAct studies under different shear rates: 1:50 diluted platelet rich plasma ($\sim 6-10 \times 10^6$ platelets/ml) was shear mixed with $10 \mu\text{g/ml}$ hV, hCV or hNV for 5 min. at various shear rates (1000-9600/s) using a cone-plate viscometer. % platelet activation was quantified based on Annexin-V binding using flow cytometry. Here, platelet activation (%) measures the fraction of platelets with exposed phosphatidylserine. Such platelets bind high amounts of FITC-conjugated Annexin-V. * $P < 0.05$ with respect to all other treatments. All proteins augment platelet activation only above 6000/s. The magnitude of platelet activation is greater upon usage of hNV.

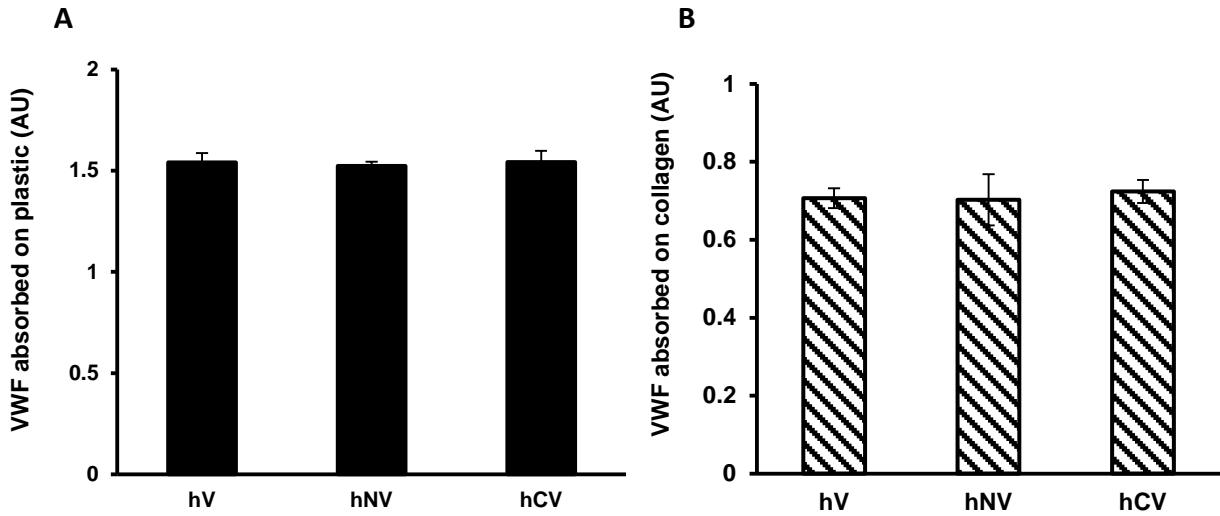


Figure S3. VWF-collagen binding. Petri dishes used for the microfluidics studies were either left uncoated (panel A) or coated with 20 μ g/mL equine type I collagen (panel B) overnight at 4 $^{\circ}$ C. The dishes were then washed. In panel A, 10 μ g/mL VWF was added to the dishes at room temperature for 1h prior to blocking with 1% BSA. In panel B, the dishes were first blocked with BSA prior to the addition of 10 μ g/mL VWF for another hour. VWF bound to these substrates was quantified using horse-radish peroxidase (HRP) conjugated polyclonal anti VWF Ab (Dako) and o-phenylenediamine (OPD) substrate. All VWF constructs bind plastic and collagen to an equal extent.

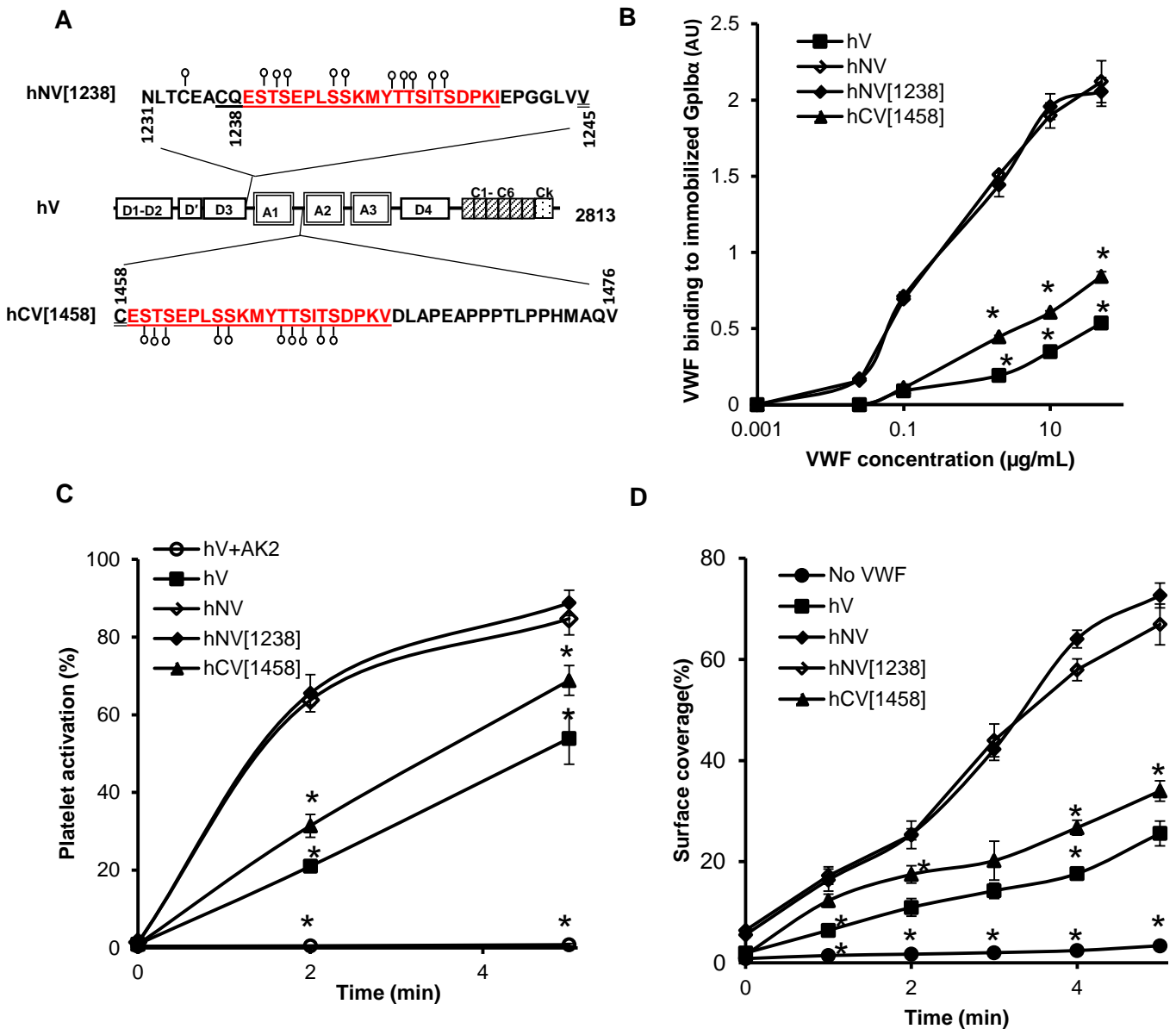


Figure S4. Functional studies with human VWF containing mucin-inserts following aa1238 at the N-terminus of VWF-A1 and aa1458 at the C-terminus of A1. **A.** The 22 amino acid mucin-insert from human CD43 (underlined) was inserted after aa1238 to generate the VWF-variant 'hNV[1238]'. Insertion of the same sequence between Cys1458 and Asp1459 resulted in 'hCV[1458]'. **B.** Binding of different concentrations of VWF variants to 4 $\mu\text{g}/\text{mL}$ immobilized Gplb α -Fc in microtiter plates. **C.** SIPAct studies were performed by shearing $10^7/\text{mL}$ CD31-labeled washed platelets with $10\mu\text{g}/\text{mL}$ recombinant VWF variants at 9600s^{-1} ($100\text{ dyn}/\text{cm}^2$ shear stress) in a cone-plate viscometer. AK-2 is an anti-Gplb α blocking mAb. **D.** $10^8/\text{mL}$ BCECF-labeled fluorescent human platelets were resuspended in plasma-free blood supplemented with $10\mu\text{g}/\text{mL}$ recombinant human VWF variants. The mixture was perfused over equine collagen bearing substrates for 5 min at a wall shear rate of 1000 s^{-1} (Shear stress of $40\text{ dyn}/\text{cm}^2$). Thrombus formation quantified the percentage of substrate covered by platelets. Control runs were plasma-free without addition of VWF. * $P < 0.05$ with respect to all other treatments. hNV[1238] function was very similar to hNV, and it displayed significantly higher binding to platelets compared to either normal VWF (hV) or mutant with C-terminal mucin insert (hCV[1458]).

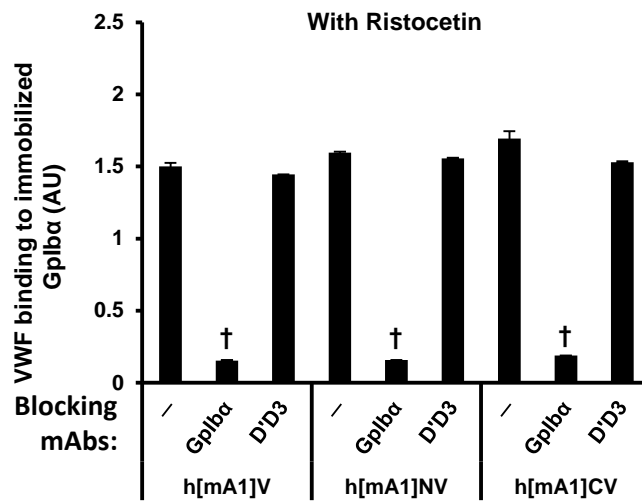


Figure S5. Chimeric VWF binding to Gplb α in the presence of ristocetin. 4 μ g/ml Gplb α -Fc was immobilized in microwell plates. 10 μ g/ml chimeric VWF variants were added in the absence or presence of 20 μ g/mL blocking antibody (AK2 for GPIb α or DD3.1 for VWF-D'D3) and 1.5 mg/mL ristocetin. VWF binding was quantified using horse-radish peroxidase (HRP) conjugated polyclonal anti-VWF Ab (Dako) and OPD substrate. All data are from 3-4 independent runs with each run having 2-3 repeats. † $P < 0.05$ with respect to all other treatments.

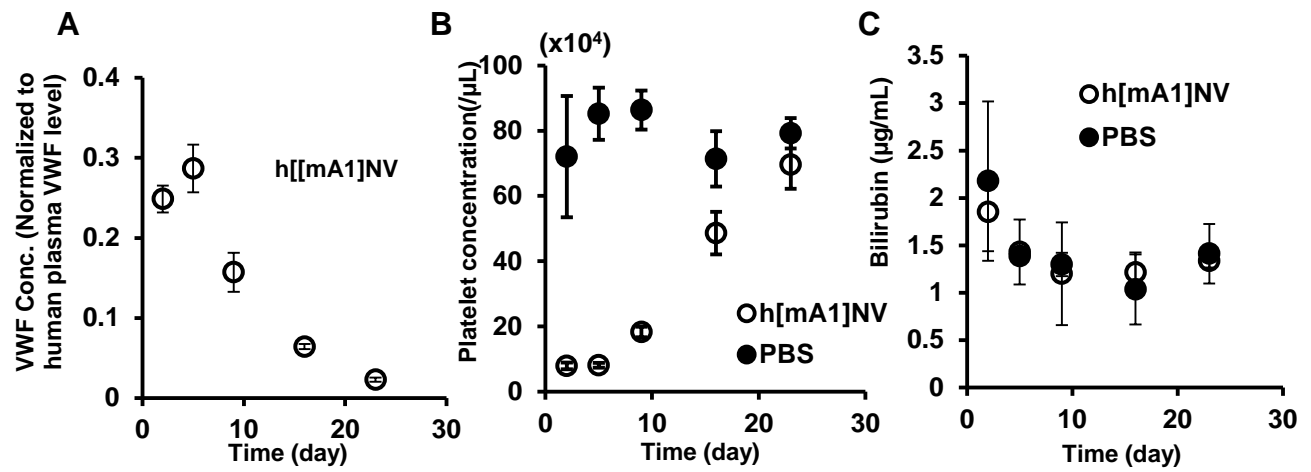


Figure S6. Time course of VWF expression and platelet counts following h[mA1]NV hydrodynamic injection. Hydrodynamic injection was performed either with vector carrying h[mA1]NV or PBS/vehicle control (protocol in Fig. 5, main manuscript). Various measurements were made at defined times: **A:** Chimeric VWF concentrations in mouse plasma measured with respect to human VWF standards prepared by pooling plasma from 5 healthy donors; **B:** Platelet counts; **C:** Bilirubin level. Platelet concentration was depressed for 7-10 days. Plasma bilirubin levels did not change dramatically. All mice recovered normally at the end.

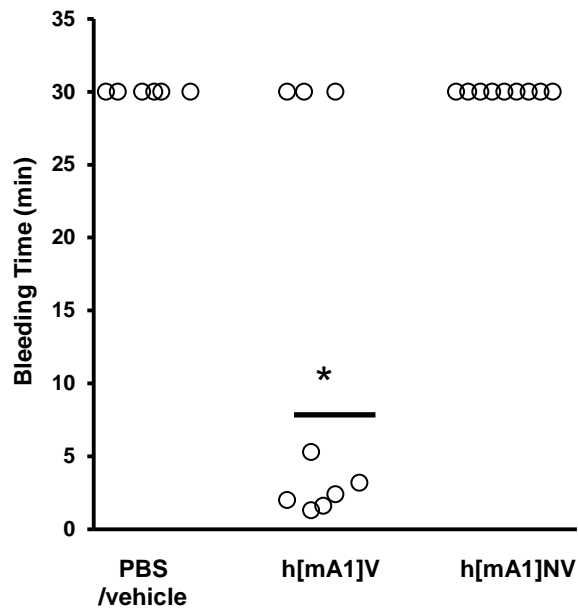


Figure S7. Tail bleeding time. Bleeding time was measured from the moment of tail transection until first arrest of bleeding. Observations were stopped at 30min when bleeding did not cease. h[mA1]V typically corrected bleeding defect observed in VWF^{-/-} (PBS/vehicle injection). Bleeding was not corrected in 3/9 mice perhaps due to variable protein expression following hydrodynamic injection. Bleeding in h[mA1]NV was unabated, typically at levels greater than even the vehicle/PBS VWF^{-/-} mouse. * $P < 0.05$ with respect to all other treatments.

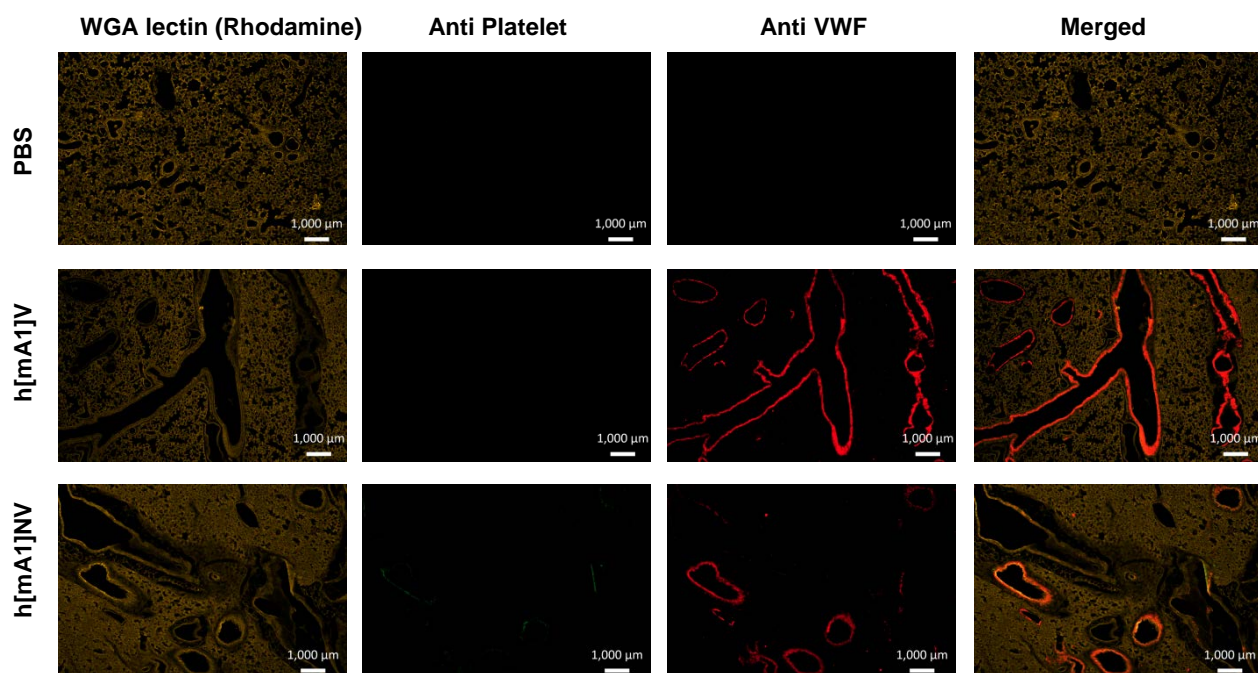


Figure S8. Immunohistochemical staining of lung section. Besides the liver, hydrodynamic injection of h[mA1]V and h[mA1]NV also resulted in protein expression in lung (third column), though there was no platelet accumulation in this organ (second column). All images were captured identically to Fig. 5 (main manuscript).

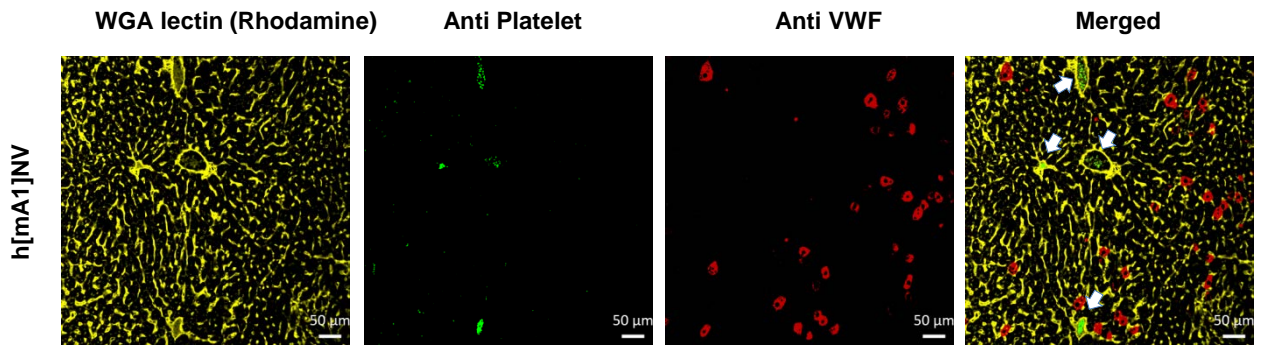


Figure S9. VWF expression and platelet thrombosis in liver. Additional examples of thrombosis (white arrow) in the liver sections upon h[mA1]NV hydrodynamic injection. All sections were prepared following perfusion fixation. Methods and results are same as Fig. 5 (main manuscript).

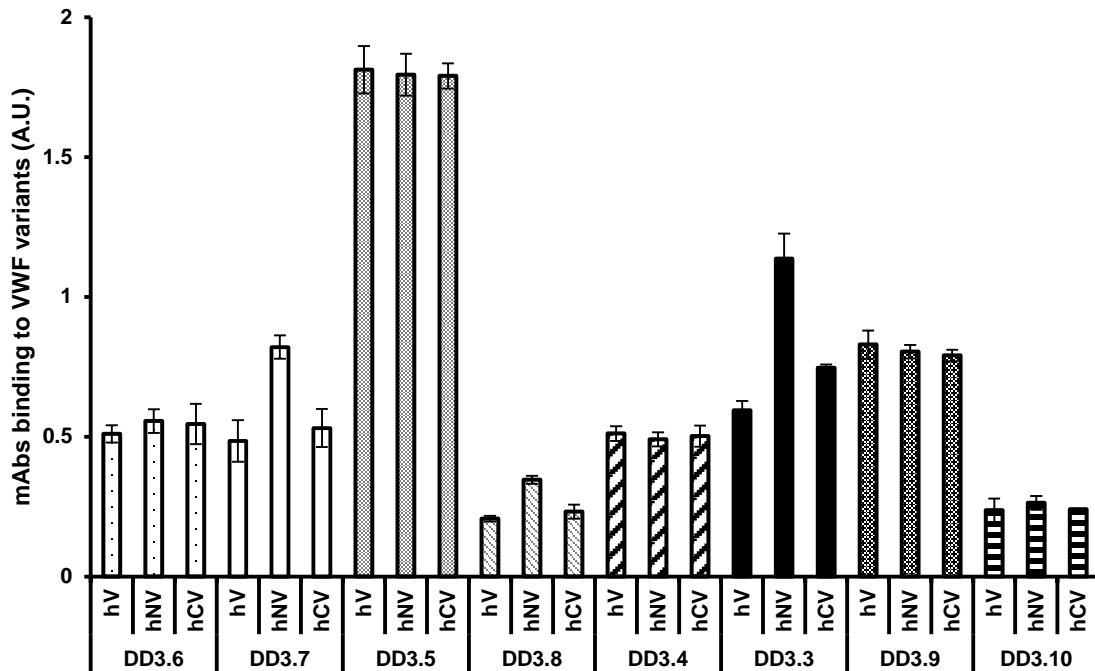


Figure S10. Conformational sensitive mAb screening. 10 μ g/mL human VWF variants (hV, hNV or hCV) were physisorbed on 96-well plates overnight. Following blocking, various anti-D'D3 clones were added to the wells for 30min using standard ELISA methods. The extent of mAb binding to absorbed human VWF variants was measured using goat-anti-mouse HRP to identify anti-D'D3 mAbs that bind differentially to the immobilized proteins. DD3.3 reproducibly bound hNV better than hCV or hV.

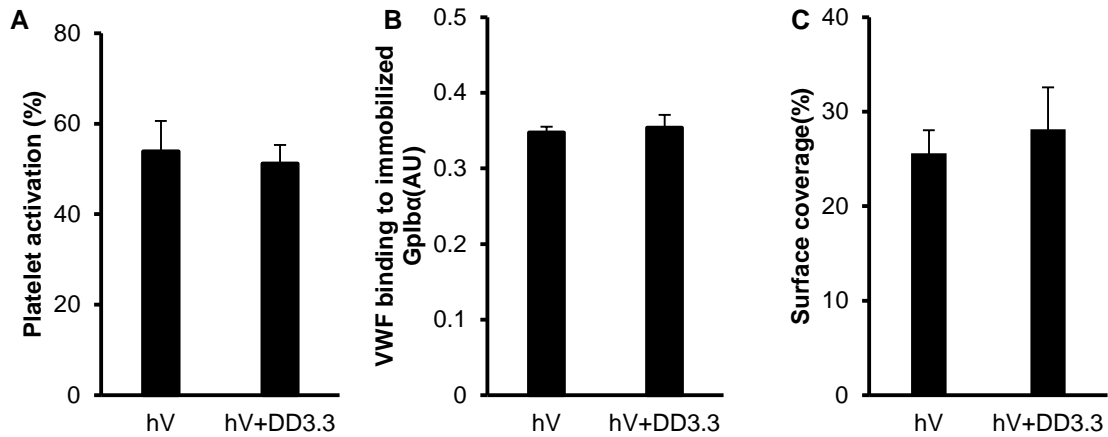


Figure S11. DD3.3 is a non-function blocking mAb. Studies were performed to confirm that DD3.3 does not block shear-induced platelet activation (SIPA, panel **A**), VWF binding to immobilized GpIb α -Fc in ELISA (panel **B**) or thrombus formation under shear (panel **C**). In all studies, 20 μ g/ml DD3.3 antibody was added to VWF at least 10 min prior to the functional assay. All experiments followed protocols described in the main manuscript.